Electronic Supplementary Material (ESI) for RSC Advances. This journal is © The Royal Society of Chemistry 2022

Electronic Supplementary Information

Sequential detection of hypochlorous acid and sulfur dioxide derivatives by a red-emitting fluorescence probe and bioimaging application *in vitro* and *in vivo*

Jianhua Liu,‡[a,c] Haoyuan Yin,‡[a] Zhuye Shang,[a] Pengli Gu,[b] Guangjie He,[b]* Qingtao Meng,[a]* Run Zhang[d] and Zhiqiang Zhang[a]*

[a] School of Chemical Engineering, University of Science and Technology Liaoning, Anshan, Liaoning Province, 114051, P. R. China.

E-mail:qtmeng@ustl.edu.cn, zzq@ustl.edu.cn; Tel: +86-412-5929627

[b] School of Forensic Medicine, Xinxiang Medical University, 601 Jinsui Road, Xinxiang, 453003, Henan Province, P. R. China.

E-mail: guangjiehe@163.com

[c] College of pharmacy, Jilin Medical University, Jilin, Jilin Province, 132001, P. R. China.

[d] Australian Institute for Bioengineering and Nanotechnology, The University of Queensland, Brisbane, 4072, Australia

‡ These authors contributed equally to this work and they should be regarded as co-first authors.

Instruments

^{1}H NMR and ^{13}C NMR spectra were both collected on an AVANCE600MHZ spectrometer (BRUKER) with chemical shifts reported as *ppm* (in DMSO, TMS as internal standard). Coupling constants (*J* values) are reported in hertz. API mass spectra were recorded on an Agilent 6530 QTOF spectrometer. Absorption spectra were measured with a Perkin Elmer Lambda 900 UV/VIS/NIR spectrophotometer (USA). Fluorescence spectra were measured with Perkin Elmer LS55 luminescence spectrometer (USA). All pH measurements were made with an OHAUS Starter 3100/f meter (USA). Fluorescent live cell images were recorded on a Nikon A1 inverted confocal laser-scanning microscope. Fluorescence imaging in adult zebrafish and mice were imaged by a SPECTRAL Ami Imaging Systems (Spectral Instruments Imaging, LLC, Tucson, AZ) with an excitation filter 465 nm and an emission filter 610 nm. All the data were calculated using the region of interest (ROI) function of Amiview Analysis software (Version 1.7.06), and values are presented as the mean ± SD for each group of three experiments.

Materials

Phenothiazine, 3-hydroxy-3-methylbutanone, malononitrile were purchased from Aladdin reagent Co. (Shanghai, China).1-Bromopropane, piperidine, phosphorus oxychloride, sodium ethoxide, metal ions (nitrate salts), and anions (sodium salts) were obtained from Sinopharm Chemical Reagent Co., Ltd. (China). 3-Morpholinosydnonimine (SIN-1) ($ONOO^-$ donor) and sodium hypochlorite (NaOCl) were purchased from Sigma Aldrich. Fetal bovine serum (FBS), L-glutamine,

penicillin, dulbecco's Modified Eagle Medium (DMEM), streptomycin sulfate and trypsin-EDTA were purchased from Life Technologies (Australia). Adult zebrafish and nude mice were commercially available. All the experiments of live zebrafish and nude mice were performed in compliance with the relevant local laws and institute guidelines. Unless otherwise stated, solvents and reagents were of analytical grade from commercial suppliers and were used without further purification. Deionized water was used throughout.

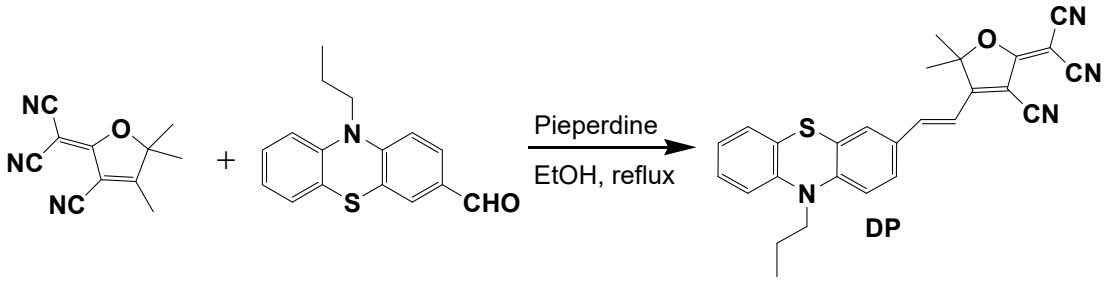

Scheme S1 Synthetic procedure of the fluorescence probe **DP**.

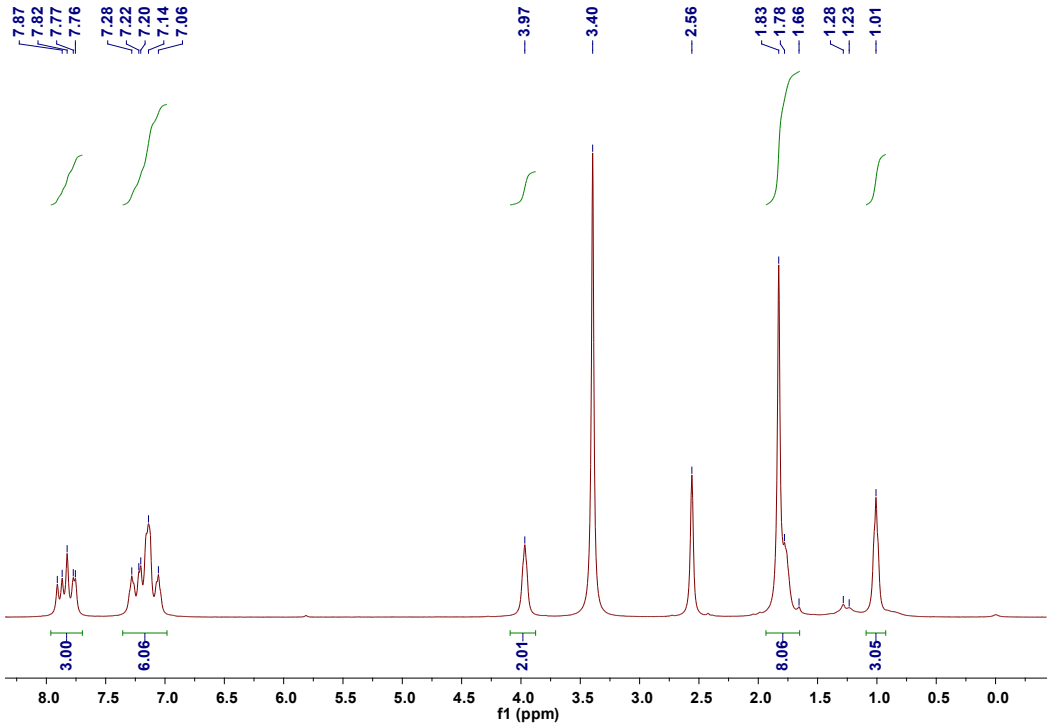

Fig. S1 ^{1}H NMR of Probe **DP** (DMSO-d_6).

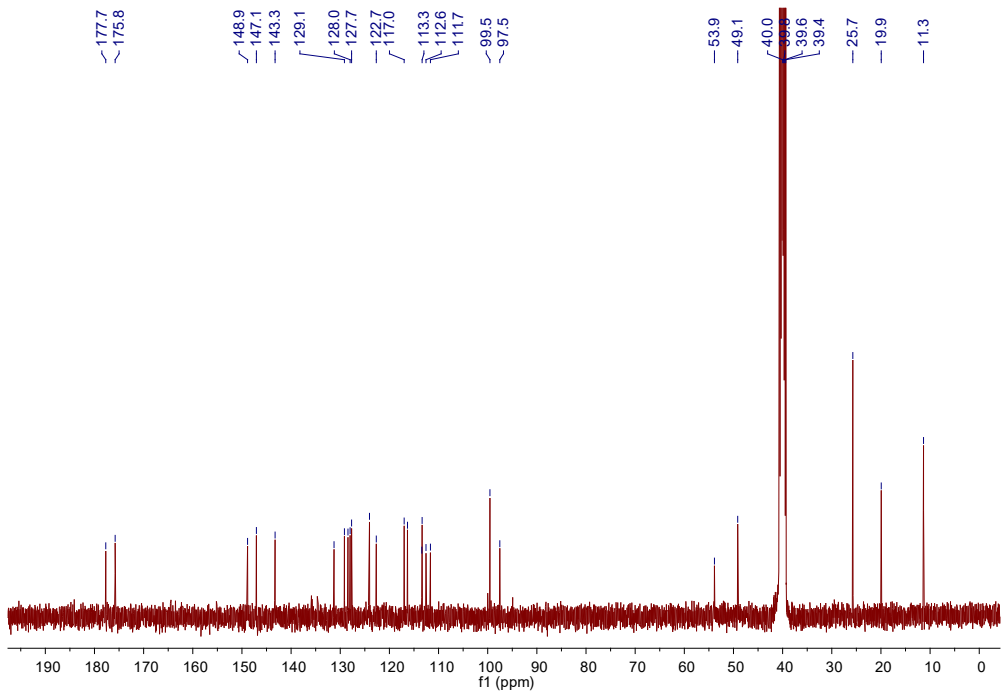

Fig. S2 ^{13}C NMR of Probe **DP** (DMSO-d_6).

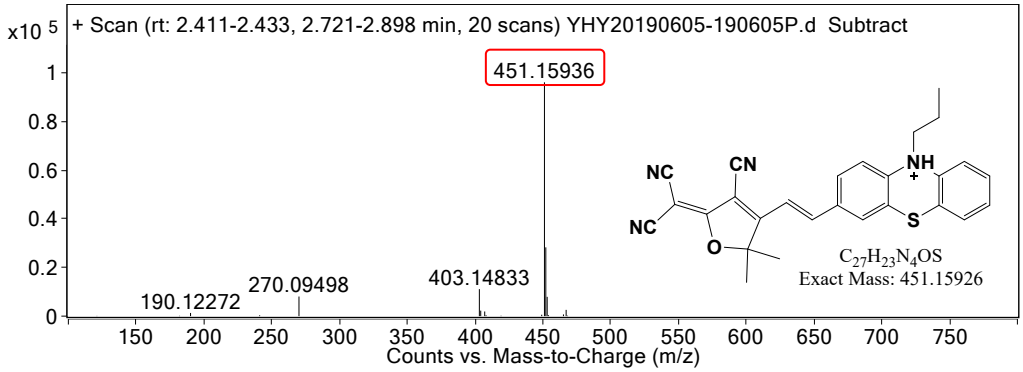

Fig. S3 HRMS of Probe **DP**.

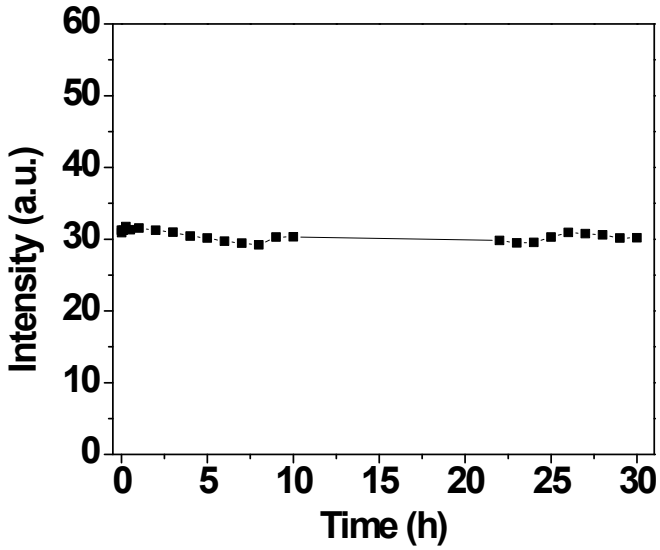

Fig. S4 Fluorescence spectra of Probe **DP** (10 μM) in PBS aqueous buffer (DMF: H_2O=1:9, v:v, 20 mM, pH=7.4). Excitation was performed at 480 nm.

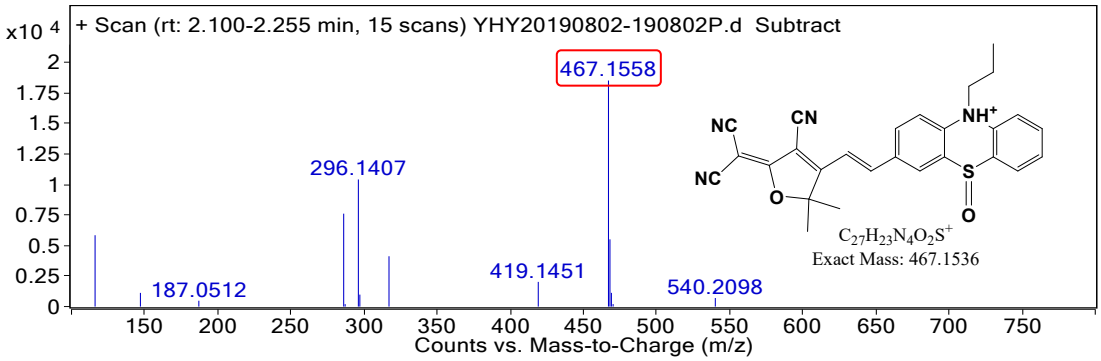

Fig. S5 HRMS of Probe **DP** in the presence of HOCl.

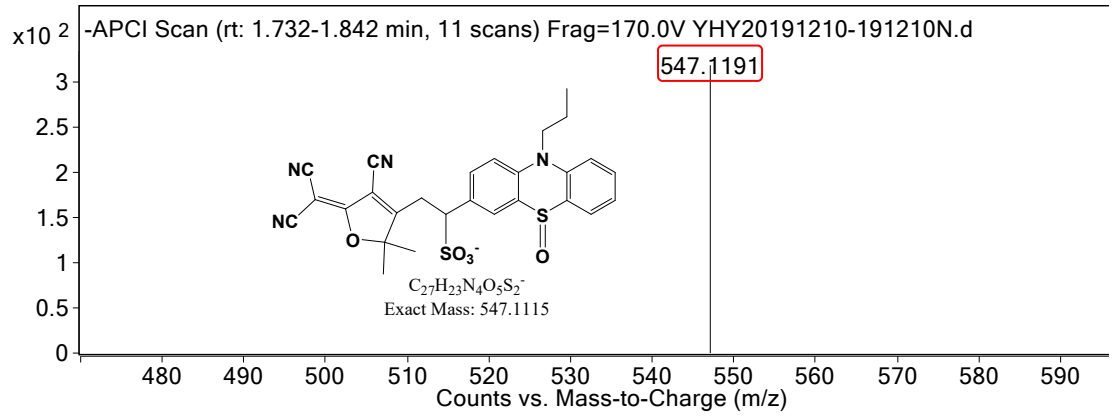

Fig. S6 HRMS of **DP=O** in the presence of HSO_3^-.

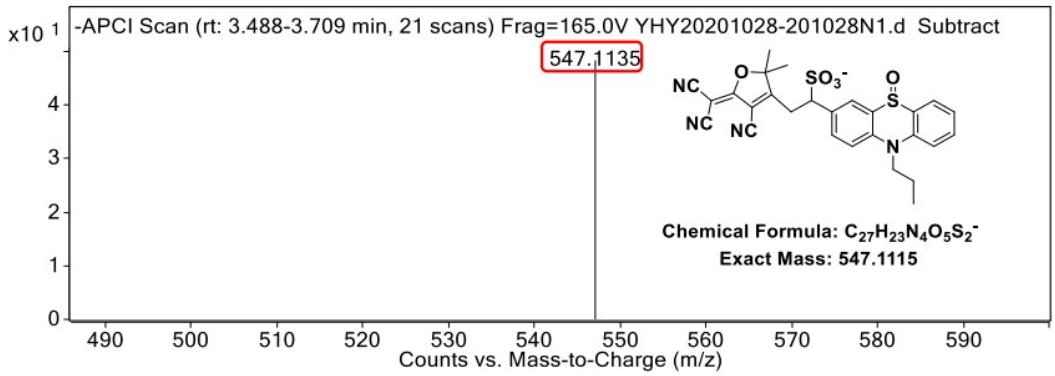

Fig. S7 HRMS of **DP=O** in the presence of SO_3^{2-}.

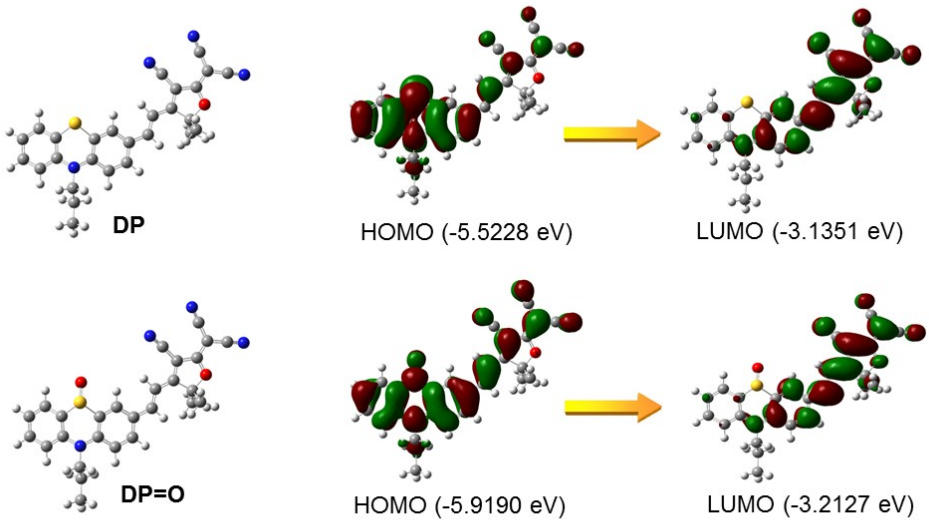

Fig. S8. Theoretical computations of **DP** and **DP=O**. Optimized molecular geometries of **DP** and **DP=O**, HOMO and LUMO orbital distributions, and the corresponding electric energies.

Table S1. Cartesian coordinates of **DP** in the ground state (S_0).

Coordinates (ground state S_0)

Center Number	Atomic Number	Forces (Hartrees/Bohr) X	Y	Z
1	6	0.000007314	0.000003141	0.000000217
2	6	-0.000013613	-0.000002267	-0.000001886
3	6	0.000010293	0.000004836	0.000001392
4	6	-0.000003409	-0.000014392	0.000000239
5	6	-0.000001934	0.000008541	0.000006157
6	6	-0.000002990	-0.000002776	-0.000002596
7	16	-0.000000759	0.000002844	0.000000681
8	6	0.000008623	-0.000014066	0.000000347
9	6	-0.000022911	0.000020387	0.000013848
10	7	0.000018879	-0.000016558	-0.000025301
11	6	-0.000008076	0.000003250	0.000002226
12	6	0.000003719	0.000006104	0.000001431
13	6	0.000000677	-0.000006693	0.000001159
14	6	-0.000000072	-0.000003105	-0.000002030
15	6	0.000000289	0.000007681	0.000013756
16	6	0.000000877	0.000001753	-0.000003956
17	6	0.000000723	0.000000282	-0.000001018
18	6	0.000006371	0.000003297	0.000001211
19	6	-0.000005580	-0.000002852	-0.000002067
20	6	0.000005088	0.000001741	0.000001102
21	6	-0.000006079	-0.000001584	-0.000000206
22	6	-0.000015861	0.000016490	-0.000000936
23	8	0.000008264	-0.000010875	-0.000001272
24	6	0.000002936	-0.000001528	-0.000001247
25	6	0.000004395	-0.000000149	0.000003820
26	6	0.000009753	-0.000002431	-0.000002037
27	7	-0.000001142	0.000001344	0.000002252
28	6	-0.000002959	0.000000098	-0.000000595
29	6	-0.000000834	0.000000155	-0.000000698

30	6	-0.000010588	0.000004894	-0.000009122
31	7	0.000001031	-0.000000221	0.000003087
32	6	0.000006353	-0.000001434	0.000001645
33	7	-0.000002022	0.000001022	-0.000000127
34	1	-0.000001201	-0.000000333	-0.000000820
35	1	-0.000001820	-0.000000977	0.000002092
36	1	0.000002074	0.000000409	0.000000548
37	1	0.000001278	-0.000001049	0.000002744
38	1	-0.000000522	-0.000001937	0.000000655
39	1	0.000000624	0.000000111	0.000001550
40	1	0.000001010	-0.000000491	0.000001113
41	1	-0.000001589	-0.000002167	-0.000001506
42	1	0.000000083	-0.000000928	-0.000000242
43	1	0.000000284	-0.000002002	0.000001341
44	1	0.000000336	0.000000799	0.000000678
45	1	0.000000308	-0.000000690	-0.000000591
46	1	0.000000113	-0.000000258	-0.000000616
47	1	0.000001037	-0.000000580	-0.000000311
48	1	0.000000389	0.000000523	0.000001908
49	1	0.000000761	0.000000905	-0.000000165
50	1	-0.000000874	-0.000001240	-0.000001323
51	1	0.000000792	-0.000000189	-0.000000507
52	1	-0.000000071	0.000000823	-0.000002162
53	1	0.000001070	0.000001337	-0.000001276
54	1	-0.000000604	0.000000542	-0.000001642
55	1	-0.000000232	0.000000461	-0.000000938

Table S2. Cartesian coordinates of **DP=O** in the ground state (S_0).

Coordinates (ground state S_0)

Center Number	Atomic Number	Forces (Hartrees/Bohr) X	Y	Z
1	6	-0.000002786	0.000001771	-0.000000558
2	6	0.000002557	-0.000009000	0.000004082
3	6	-0.000010733	0.000009478	-0.000002619
4	6	0.000006268	-0.000025357	-0.000002134
5	6	-0.000005350	0.000022658	-0.000004626
6	6	0.000007731	-0.000002873	0.000001119
7	16	-0.000004037	0.000018603	0.000001748
8	6	0.000002492	-0.000019910	0.000003024
9	6	-0.000004548	0.000013891	0.000004824
10	7	-0.000001824	-0.000009330	0.000000322
11	6	0.000003981	0.000008656	-0.000000085
12	6	-0.000000577	-0.000008860	0.000006005
13	6	-0.000000651	0.000004005	0.000005882
14	6	0.000000157	-0.000004901	0.000001779
15	6	0.000002435	0.000003880	-0.000004180
16	6	-0.000001824	-0.000000668	0.000004354
17	6	0.000000691	-0.000005654	-0.000004206
18	6	-0.000000364	0.000003762	-0.000002334
19	6	0.000002034	-0.000001265	-0.000000017
20	6	-0.000001256	0.000001290	0.000001446
21	6	0.000003446	-0.000001233	0.000005463
22	6	0.000008006	-0.000001635	0.000000593
23	8	-0.000002365	0.000004066	-0.000001638

24	6	-0.000003024	-0.000001331	-0.000004780
25	8	0.000000377	-0.000000370	0.000008179
26	6	-0.000006603	-0.000006194	-0.000000239
27	6	-0.000006055	0.000002424	0.000001191
28	7	-0.000000406	0.000000691	0.000005499
29	6	0.000002628	-0.000000446	-0.000000799
30	6	-0.000000036	0.000001780	-0.000001096
31	6	0.000004134	0.000003039	0.000005606
32	7	0.000000714	-0.000001209	-0.000002397
33	6	0.000001280	0.000002343	0.000003417
34	7	-0.000001916	-0.000000129	0.000005150
35	1	-0.000000046	0.000001067	-0.000003746
36	1	0.000001210	-0.000000115	0.000004030
37	1	0.000000340	0.000003942	-0.000003165
38	1	-0.000000428	-0.000001373	0.000007499
39	1	0.000001166	-0.000000559	0.000004728
40	1	0.000001907	-0.000002496	0.000001844
41	1	0.000000373	-0.000000498	0.000000222
42	1	-0.000005042	-0.000002258	-0.000003303
43	1	0.000004967	-0.000001712	-0.000001626
44	1	0.000001005	-0.000000247	-0.000002979
45	1	-0.000000204	-0.000000218	-0.000005667
46	1	0.000001874	-0.000001192	-0.000006410
47	1	0.000000042	0.000000822	-0.000005270
48	1	0.000000478	0.000001484	-0.000004101
49	1	-0.000000578	-0.000000144	-0.000002501
50	1	-0.000000566	0.000000260	0.000000061
51	1	0.000001872	-0.000000842	-0.000003080
52	1	0.000001777	-0.000002716	-0.000002359
53	1	0.000000666	-0.000000925	-0.000003851
54	1	-0.000001948	0.000002045	-0.000002889
55	1	-0.000001538	0.000001616	-0.000004158
56	1	-0.000001898	0.000002086	-0.000001257

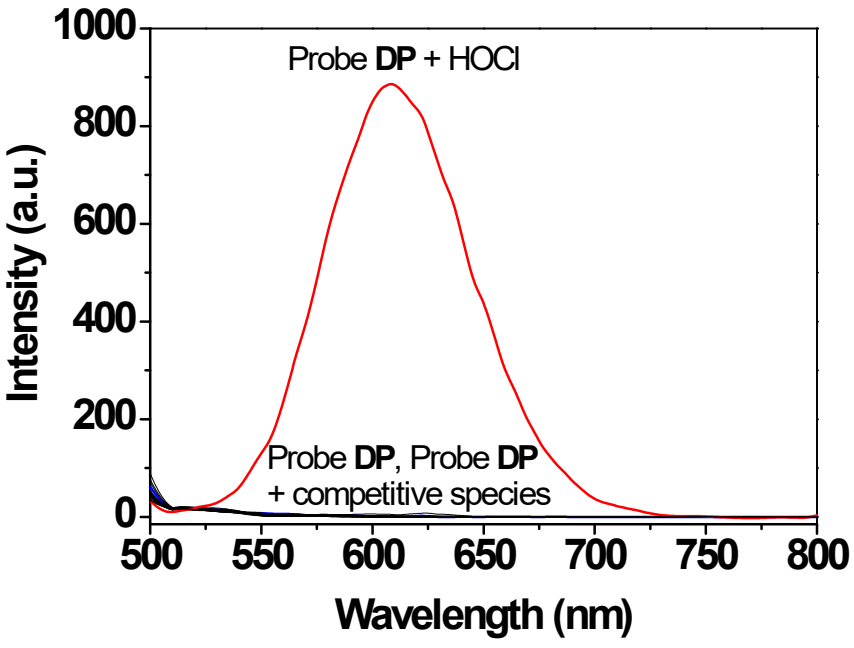

Fig. S9 Fluorescence responses of Probe **DP** (10 μM) to various analytes (60 μM) in PBS aqueous buffer (DMF: H_2O=1:9, v:v, 20 mM, pH=7.4), excitation at 480 nm.

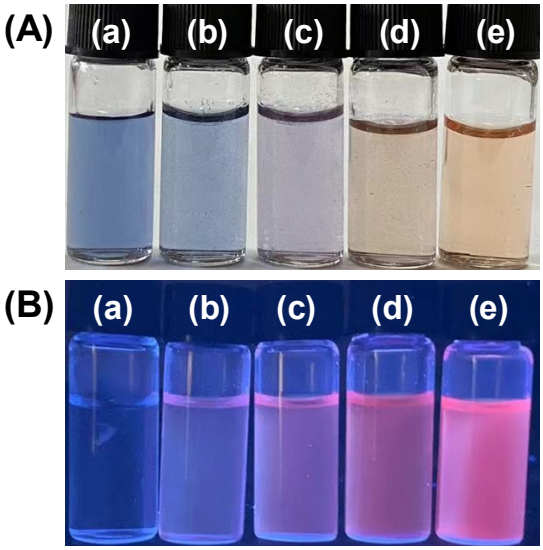

Fig. S10. (A) Color responses of **DP** (10 μM) towards HOCl in PBS aqueous buffer (DMF:H_2O=1:9, v:v, 20 mM, pH=7.4). (B) Fluorescence color photos of **DP** (10 μM) in the presence of HOCl in PBS aqueous buffer (DMF:H_2O=1:9, v:v, 20 mM, pH=7.4) under UV light (365 nm). (a) 0 μM, (b) 10 μM, (c) 20 μM, (d) 40 μM, (e) 60 μM.

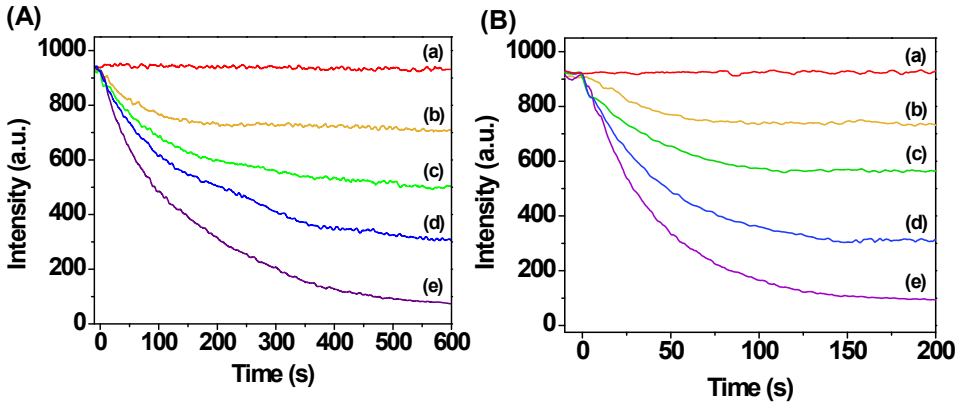

Fig. S11 (A) Time-profile fluorescence quenching at 608 nm of **DP=O** in the presence of (a) 0 μM, (b) 10 μM, (c) 15 μM, (d) 20 μM, (e) 30 μM SO_3^{2-} in PBS aqueous buffer (DMF: H_2O=1:9, v:v, 20 mM, pH=7.4). (B) Time-profile fluorescence quenching at 608 nm of **DP=O** in the presence of (a) 0 μM, (b) 10 μM, (c) 20 μM, (d) 30 μM, (e) 50 μM HSO_3^-in PBS aqueous buffer (DMF: H_2O=1:9, v:v, 20 mM, pH=7.4). Excitation was performed at 480 nm.

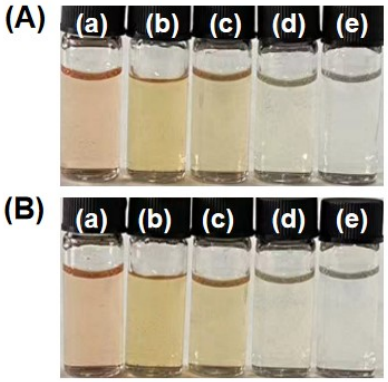

Fig. S12. Color responses of **DP=O** (10 μM) towards different concentrations of (A) SO_3^{2-} and (B) HSO_3^- in PBS aqueous buffer (DMF:H_2O=1:9, v:v, 20 mM, pH=7.4). (a) 0 μM, (b) 10 μM, (c) 20 μM, (d) 30 μM and (e) 40 μM.

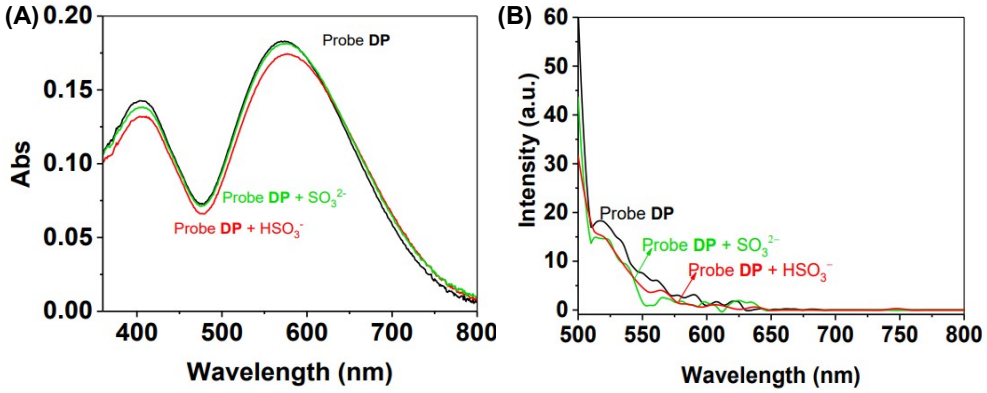

Fig. S13 (A) UV-vis absorption and (B) emission spectra of **DP** (10 μM) in the presence amounts of SO_3^{2-} (60 μM) and HSO_3^- (60 μM) in PBS aqueous buffer (DMF: H_2O=1:9, v:v, 20 mM, pH=7.4).

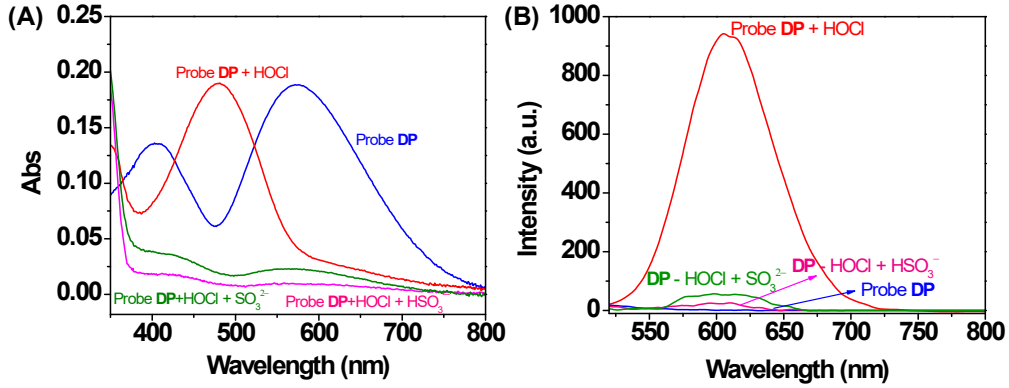

Fig. S14 (A) UV-vis absorption and (B) emission spectra of Probe **DP** (10 μM) to HOCl (60 μM) and **DP=O** to SO_3^{2-} (60 μM) and HSO_3^- (60 μM) in PBS aqueous buffer (DMF: H_2O=1:9, v:v, 20 mM, pH=7.4). Excitation at 480 nm.

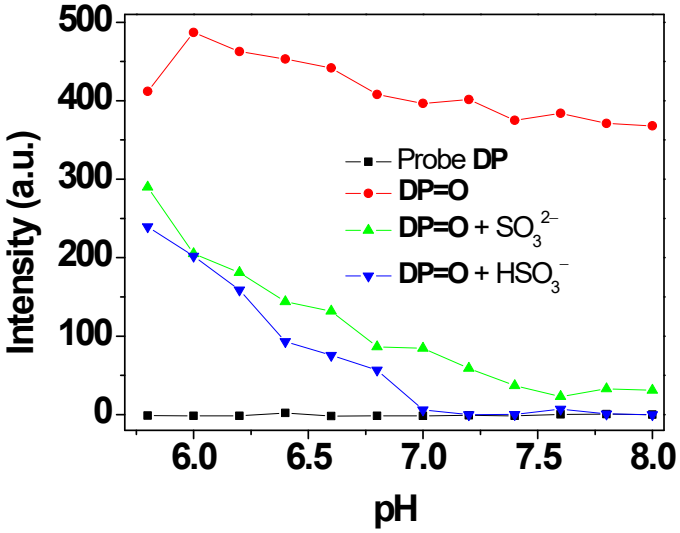

Fig. S15 Fluorescence spectra of **DP=O** (10 μM) upon the addition SO_3^{2-} (60 μM) and HSO_3^- (60 μM) in PBS aqueous buffer (DMF: H_2O=1:9, v:v, 20 mM, pH=7.4). Excitation at 480 nm.

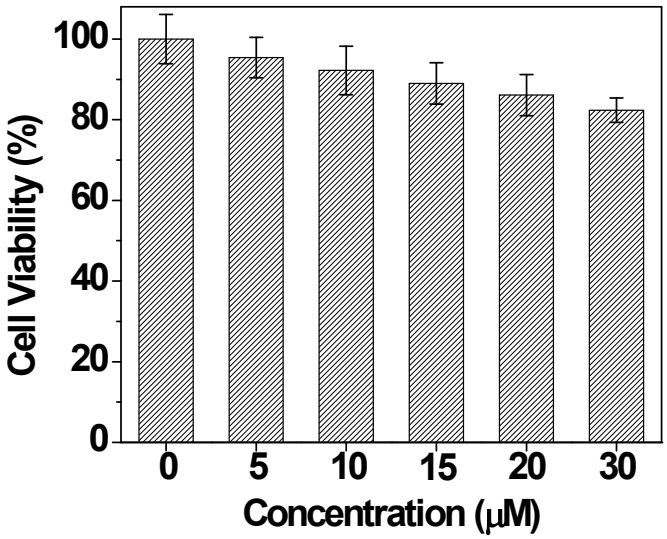

Fig. S16 The viability of A549 cells incubated with **DP** (0-30 μM) for 24 h.

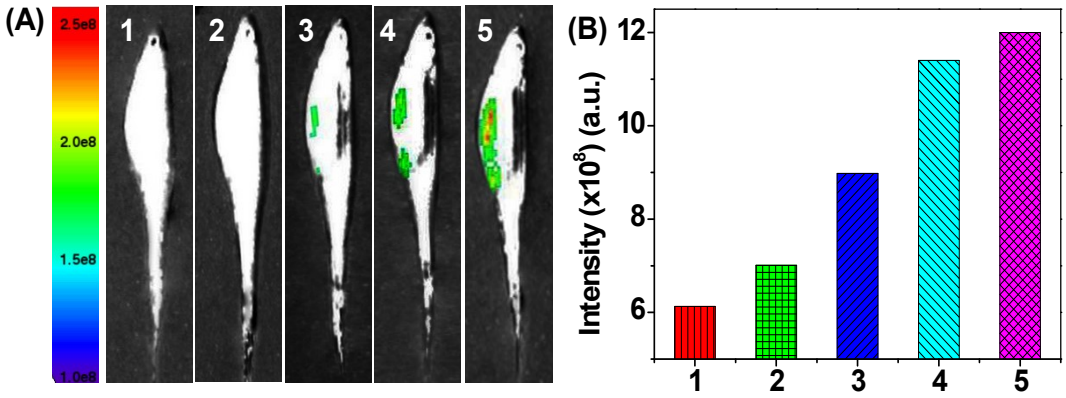

Fig. S17 (A) Fluorescence imaging of endogenous HOCl production in zebrafish. (a) Zebrafish only; (b) Zebrafish was stimulated with LPS (2 μL/mL) for 3 h; then stained with **DP** (10 μM) for

(c) 5 min (d) 10 min (e) 15 min. (B) The mean fluorescence intensities of areas of interest at different time period showing in (a-e). The zebrafish were imaged with an excitation filter (465 nm) and the emission filter (610 nm). Zebrafish were imaged with an excitation filter (465 nm) and an emission filter (610 nm).

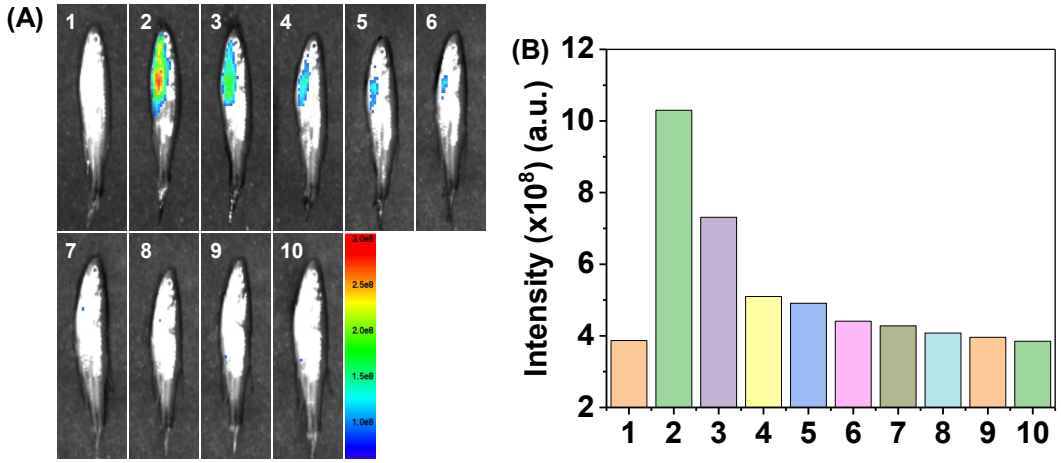

Fig. S18 (A) Fluorescence imaging of exogenous HSO_3^- in zebrafish. (1) Zebrafish only; (2) zebrafish was stimulated with **DP=O** (10 μM) for 0.5 h, (3) then stained with HSO_3^- (40 μM) for 5 min, (4) 10 min, (5) 15 min, (6) 20 min, (7) 25 min, (8) 30 min, (9) 35 min and (10) 40 min, respectively. (B) The mean fluorescence intensities of areas of interest at different time showing in (1-10). Zebrafish were imaged with an excitation filter (465 nm) and an emission filter (610 nm).

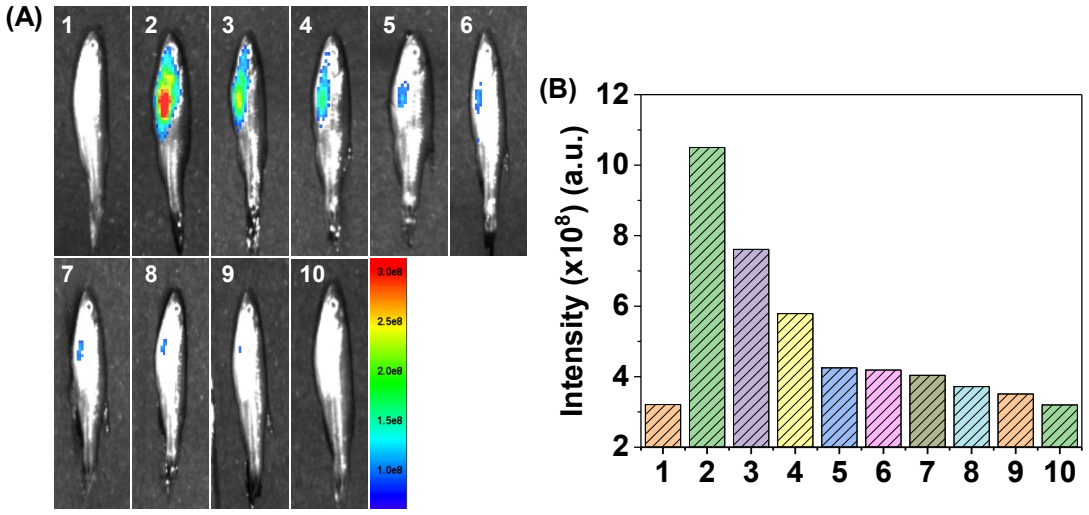

Fig. S19 (A) Fluorescence imaging of exogenous SO_3^{2-} in zebrafish. (1) Zebrafish only; (2) zebrafish was stimulated with **DP=O** (10 μM) for 0.5 h. (3) then stained with SO_3^{2-} (40 μM) for 5 min, (4) 10 min, (5) 15 min, (6) 20 min, (7) 25 min, (8) 30 min, (9) 35 min and (10) 40 min, respectively. (B) The mean fluorescence intensities of areas of interest at different time showing in (1-10). Zebrafish were imaged with an excitation filter (465 nm) and an emission filter (610 nm).

Table S3. Comparison of this work with reported fluorescent probes for the detection of HOCl and dioxide derivatives (SO_3^{2-}/HSO_3^-).

Probes	Emission wavelength	Detection of HOCl or dioxide derivatives	Detection limits	Response time	Application in live cells/ animals	Ref.
MXS	654 nm	HOCl	72 nM	30 s	HeLa cells.	1
Probe 1	520 nm	HOCl/GSH	0.237 μM for HOCl	within 2 min	HeLa cells	2
BNA-HClO	510 nm	HOCl	37.56 nM	<30 s	HOCl	3
HClO-ER	556 nm	HOCl	0.785 μM	155 s	HeLa, Raw 264.7 cells and liver tissue	4
RT-1	587 nm	HOCl	2.18×10^{-9} M	within 3 min	RAW 264.7 cells	**5**
Cou-HOCl	510 nm	HOCl	16 nM	within 5 s.	A549, HeLa and HepG 2 cells	6
JBD	607 nm	HOCl	0.067 μM	within 26 s	HeLa cells	7
MBTC	690 nm	HOCl	4.6 nM	one minute	RAW 264.7 cells	8
HDI-HClO	520 nm	HOCl	8.3 nM	within 8 s	HeLa, and RAW 264.7 cells	9
QPCT	537 nm/590 nm	HSO_3^-	0.44 μM	7 min	A549 cells	10
PCPT	568 nm/648 nm	HSO_3^-	80.5 nM	15 min	HeLa cells, L-O2 cells and HepG2 cells	11
BCVTI	608 nm	HSO_3^-	3.3 nM	4 min	No	12
HDI	460 nm/565 nm	HSO_3^-	80 nM	2 min	MCF-7 cells	13
DQ	620 nm	HSO_3^-	0.11 μM	15 s	HepG2 cells	14
CMQ	640 nm	HSO_3^-	15.6 nM	5 s	HeLa cells, Zebrafish	15
probe 1	450 nm/594 nm	HSO_3^-	3.21 μM	2.5 min	No	16
Ru-azo	635 nm	HSO_3^-	0.69 μM	60 min	No	17
MITO-TPE	455 nm	HSO_3^-	27.22 μM	20 s	MCF-7 Cells, Zebrafish	18
Hcy-Mo	596 nm	HSO_3^-	80 nM	30 s	MDA-MB-231 cells, Mouse	19

RBC	456 nm/583 nm	HSO_3^-	6.6×10^{-8} M	35 s	HeLa and HepG2 cells	20
Q5	485 nm/650 nm	HSO_3^-	89 nM	within 0.5 h	CEM cells	21
BPyn	512 nm/704 nm	HSO_3^-	0.09 μM	15 s	HeLa cells	22
Probe PBC1	458 nm/610 nm	HOCl and SO_2	13 Nm, 7 nM	within 20 s	HeLa cells, 3-day-old zebrafish	23
DNB	525 nm/600 nm for HOCl; 425 nm/600 nm for SO_2	HOCl and SO_2	8.0 nM for SO_2 and 15.2 nM for HOCl	SO_2 < 50 s, HOCl < 20 s	HeLa cells, zebrafish	24
DP	608 nm	HOCl and SO_3^{2-}/HSO_3^-	89.5 nM, 70.8 nM/65.1 nm	30 s for HOCl, 600 s for SO_3^{2-}/HSO_3^-	Live Hela cells, zebrafish and mouse	**This work**

References:

1. J. Gong, C. Liu, S. Cai, S. He, L. Zhao and X. Zeng, Novel near-infrared fluorescent probe with a large Stokes shift for sensing hypochlorous acid in mitochondria. *Org. Biomol. Chem*., 2020, **18**, 7656–7662.
2. C. Jiao, Y. Liu, W. Lu, P. Zhang, X. Ma and Y. Wang, A simple sensor based on 1,8-naphthalimide with large Stokes shift for detection of hypochlorous acid in living cells. *RSC Adv*., 2019, **9**, 31196–31201.
3. W. Hu, M. Zhao, K. Gu, L. Xie, M. Liu and D. Lu, Fluorescent probe for the detection of hypochlorous acid in water samples and cell models. *RSC Adv*., 2022, **12**, 777–784.
4. W. Zhang, W. Song and W. Lin, A novel ER-targeted two-photon fluorescent probe for monitoring abnormal concentrations of HClO in diabetic mice. *J. Mater. Chem. B*, 2021, **9**, 7381–7385.
5. M. G. Choi, Y. J. Lee, K. M. Lee, K. Y. Park, T. Jung Park and S.-K. Chang, A simple hypochlorous acid signaling probe based on resorufin carbonodithioate and its biological application. *Analyst*, 2019, 1**44**, 7263–7269.
6. Z. Xu, X. Wang, T. Duan, R. He, F. Wang and X. Zhou, Development of an ultrafast fluorescent probe for specific recognition of hypochlorous acid and its application in live cells. *RSC Adv*., 2021, **11**, 24669–24672.
7. H. Ren, F. Huo and C. Yin, An ESIPT-based colorimetric and fluorescent probe with large Stokes shift for the sensitive detection of hypochlorous acid and its bioimaging in cells. *New J. Chem*., 2021, **45,** 4724–4728.
8. J. Sun and F. Feng, An S-alkyl thiocarbamate-based biosensor for highly sensitive and selective detection of hypochlorous acid. *Analyst*, 2018, **143**, 4251–4255

9. P. Luo and X. Zhao, A Sensitive and Selective Fluorescent Probe for Real-Time Detection and Imaging of Hypochlorous Acid in Living Cells. *ACS Omega*, 2021, **6**, 12287–12292.
10. J. Lia, Y. Gao, H. Guo, X. Li, H. Tang, J. Li and Y. Guo, A novel colorimetric and ratiometric fluorescent probe for selective detection of bisulfite in real samples and living cells. *Dyes Pigments*, 2019, 1**63**, 285-290.
11. W.-X. Sun, N. Li, Z.-Y. Li, Y.-C. Yuan, J.-Y. Miao, B.-X. Zhao and Z.-M. Lin, A mitochondria-targeted ratiometric fluorescence probe for detection of SO_2 derivatives in living cells. *Dyes Pigments*, 2020, 1**82**, 108658.
12. F. Li, L. Zou, J. Xu, F. Liu, X. Zhang, H. Li, G. Zhang and X. Duan, A high-performance colorimetric fluorescence sensor based on Michael addition reaction to detect HSO_3^- in real samples. *J. Photoch. Photobio. A*, 2021, **411**, 113201.
13. L. Wang, W. Yang, Y. Song, Y. Gu and Y. Hu, A double-indole structure fluorescent probe for monitoring sulfur dioxide derivatives with distinct ratiometric fluorescence signals in mammalian cells. *Spectrochim. Act A*, 2020, **225**, 117495.
14. C. Zhang, L. Han, Q. Liu, M. Liu, B. Gu and Y. Shen, A colorimetric and far-red fluorescent probe for rapid detection of bisulfite/sulfite in full water-soluble based on biquinolinium and its applications. *Spectrochim. Acta A*, 2021, **253**, 119561.
15. X. Bao, X. Cao, Y. Yuan, B. Zhou and C. Huo, Ultrafast Detection of Sulfur Dioxide Derivatives by a Distinctive "Dual-Positive-Ion" Platform that Features a Doubly Activated but Irreversible Michael Addition Site. *J. Agric. Food Chem*., 2021, **69**, 4903–4910.
16. X. Mu, J. Zhu, L. Yan and N. Tang, A ratiometric fluorescent probe for the rapid and specific detection of HSO_3^- in water samples. *Luminescence*, 2021, **36**, 923–927.
17. W. Zhang, X. Xi, Y.-L. Wang, Z. Du, C. Liu, J. Liu, B. Song, J. Yuan and R. Zhang, Responsive ruthenium complex probe for phosphorescence and time-gated luminescence detection of bisulfite. *Dalton Trans.*, 2020, **49**, 5531–5538.
18. X. Yang, J. Tang, D. Zhang, X. Han, J. Liu, J. Li, Y. Zhao and Y. Ye, An AIE probe for imaging mitochondrial SO_2- induced stress and SO_2 levels during heat stroke. *Chem. Commun*., 2020, **56**, 13217–13220.
19. R. Zhou, G. Cui, Y. Hu, Q. Qi, W. Huang and L. Yang, An effective biocompatible fluorescent probe for bisulfite detection in aqueous solution, living cells, and mice. *RSC Adv*., 2020, **10**, 25352–25357.
20. D. Yang, X.-Y. He, X.-T. Wu, H.-N. Shi, J.-Y. Miao, B.-X. Zhao and Z.-M. Lin, A novel mitochondria-targeted ratiometric fluorescent probe for endogenous sulfur dioxide derivatives as a cancer-detecting tool. *J. Mater. Chem. B*, 2020, **8**, 5722–5728.
21. J. Zhu, F. Qin, D. Zhang, J. Tang, W. Liu, W. Cao and Y. Ye, A novel NIR fluorescent probe for the double-site and ratiometric detection of SO_2 derivatives and its applications. *New J. Chem*., 2019, **43**, 16806–16811.
22. U. Tamima, M. Santra, C. W. Song, Y. J. Reo and K. H. Ahn, A Benzopyronin-Based Two-Photon Fluorescent Probe for Ratiometric Imaging of Lysosomal Bisulfite with Complete

Spectral Separation. *Anal. Chem*., 2019, **91**, 10779−10785.

23. J. Han, S. Yang, B. Wang and X. Song, Tackling the Selectivity Dilemma of Benzopyrylium−Coumarin Dyes in Fluorescence Sensing of HClO and SO_2. *Anal. Chem*., 2021, 9**3**, 5194−5200.
24. K. Dou, G. Chen, F. Yu, Z. Sun, G. Li, X. Zhao, L. Chen and J. You, A two-photon ratiometric fluorescent probe for the synergistic detection of the mitochondrial SO_2/HClO crosstalk in cells and *in vivo*. *J. Mater. Chem. B*, 2017, **5**, 8389−8398.